Effects of COD/N ratio on soluble microbial products in effluent from sequencing batch reactors and subsequent membrane fouling

Viet Ly Quang[a], Long D Nghiem[b], Mark Sibag[a], Tahir Maqbool[a] and Jin Hur[a,*]

[a]Department of Environment & Energy, Sejong University, Seoul 05006, South Korea

[b] Centre for Technology in Water and Wastewater, University of Technology Sydney, NSW 2007, Australia

Revised Manuscript Submitted to *Water Research*, December, 2017

* Corresponding author:

Tel. +82-2-3408-3826;

Fax +82-2-3408-4320.

E-Mail: jinhur@sejong.ac.kr

Abstract

The relative ratios of chemical oxygen demand (COD) to nitrogen (N) in wastewater are known to have profound effects on the characteristics of soluble microbial products (SMP) from activated sludge. In this study, the changes in the SMP characteristics upon different COD/N ratios and the subsequent effects on ultrafiltration (UF) membrane fouling potentials were examined in sequencing batch reactors (SBR) using excitation emission matrix-parallel factor analysis (EEM-PARAFAC) and size exclusion chromatography (SEC). Three unique fluorescent components were identified from the SMP samples in the bioreactors operated at the COD/N ratios of 100/10 (N rich), 100/5 (N medium), and 100/2 (N deficient). Fulvic-like (C2) and humic-like (C3) components were more abundant with N rich wastewater. The tryptophan-like component (C1) was the most depleted at the N medium condition. Greater abundances of large size biopolymer (BP) and low molecular weight neutrals (LMWN) were found under the N deficient and N rich conditions, respectively. SMPs from various COD/N exhibited a greater degree on membrane fouling following the order of 100/2 > 100/10 > 100/5. C1 and C2 had close associations with reversible and irreversible fouling, respectively, while the reversible fouling potential of C3 depended on the COD/N ratios. No significant impact of COD/N ratio was observed on the relative contributions of SMP size fractions to either reversible or irreversible fouling potential. However, the COD/N ratios likely altered the BP foulants' composition with greater contribution of proteinaceous substances to reversible fouling under the N deficient condition than at other N richer conditions. The opposite trend was observed for irreversible fouling. Our results provided further insight into changes in different SMP

constitutes and their membrane fouling in response to microbial activities under different COD/N ratios.

Keywords: EEM-PARAFAC; membrane fouling; size exclusion chromatography (SEC); ultrafiltration (UF); soluble microbial products (SMP), COD/N ratio

1 Introduction

Significant attention has been paid to the reclamation of municipal and industrial wastewater to address water shortages. Reclaimed water can be used for a range of applications including agricultural irrigation, industrial processing, and replenishment of potable water resources (Michael-Kordatou et al. 2015). Membrane filtration processes such as ultrafiltration (UF) have occupied a pivotal position for many of these applications given their ability to complement biological treatment in removing pathogenic agents and dissolved organic matter (DOM) (Ayache et al. 2013, Chon et al. 2012, Guo et al. 2012, Villacorte et al. 2015). However, membrane fouling caused by DOM is still a major obstacle to cost-effective UF operation. The extent of membrane fouling has been established as directly governed by the chemical composition and concentration of DOM in the feed solution (Guo et al. 2012, Maeng et al. 2015).

Effluent DOM mainly consists of soluble microbial products (SMP) formed during biological treatment (Jarusutthirak and Amy 2007, Michael-Kordatou et al. 2015). SMP is a heterogeneous mixture of organic constituents, which can be classified into three major components, namely humic substances, polysaccharides, and proteins. They are mostly produced during biomass growth (utilization-associated products; UAPs) and/or cell lysis during biomass decay (biomass-associated products; BAP) (Michael-Kordatou et al. 2015). The characteristics of SMP are dependent upon several biological treatment parameters such as organic composition of

influent wastewater (Geyik and Çeçen 2016, Hao et al. 2016, Ye et al. 2011), solid retention time (SRT) (Esparza-Soto et al. 2011, Jarusutthirak and Amy 2007), organic loading rate (OLR) (Maqbool et al. 2017), and dissolved oxygen content (Maqbool et al. 2016).

Besides the aforementioned parameters, the ratio of chemical oxygen demand (COD) to nitrogen (COD/N) or C/N has recently emerged as a particularly important one. COD/N ratio is known to be correlated with activated sludge particle size, concentrations of extracellular polymeric substances (EPS) and SMP in the mixed liquor, and their composition with respect to proteins and polysaccharides (Hao et al. 2016, Miqueleto et al. 2010, Ye et al. 2011). The COD/N ratio in wastewater varies significantly depending on the source. Some industrial wastewaters from paper pulping, petrochemical, food processing are known to contain a high portion of organic carbon content and low nitrogen content (Hao and Liao 2015). On the other hand, municipal wastewater is usually rich in nitrogen. To date, the effects of different organic composition in influent wastewater have been only highlighted on bulk protein and/or polysaccharides as the major SMP components. Considering the heterogeneous nature of SMP, it is necessary to provide further insight into the roles that the COD/N ratio has in influencing SMP characteristics and the subsequent membrane fouling for cost-effective water reclamation. Detailed information concerning SMP composition is critical to assess of the effluent fouling propensity prior to membrane filtration. For example, despite relatively a higher chemical oxygen demand (COD) content in the effluent from BAPs compared to that from UAPs, the latter showed more severe membrane fouling potential, probably due to the difference in their chemical composition (Tian et al. 2011).

Optical techniques, such as UV-Vis and fluorescence spectroscopy, have been widely applied to track the fate of different light-absorbing moieties of DOM in wastewater treatment

(Henderson et al. 2009, Li and Hur 2017). Several advanced techniques have been recently developed to provide a more detailed characterization of DOM. A notable technique is fluorescence excitation emission matrix coupled with parallel factor analysis (EEM-PARAFAC). EEM-PARAFAC is superior over other optical methods for tracking specific fluorescent DOM components in the effluent of a biological treatment process (Ishii and Boyer 2012). Several recent studies have utilized EEM-PARAFAC to reveal valuable information regarding the changes in the chemical composition of SMP in effluents from sequencing batch reactor (SBR) systems under different operation conditions (Esparza-Soto et al. 2011, Ni et al. 2009, Ni et al. 2010, Yu et al. 2015). The most powerful merit of using fluorescence spectroscopy is the ability to be further developed into an on-line monitoring system for on-site facilities since this technique is fast, non-destructive and high sensitive (Henderson et al. 2009).

Despite being very powerful, EEM-PARAFAC can only characterize light-absorbing DOM constituents. This limitation can be alleviated by using size exclusion chromatography (SEC) equipped with an organic carbon detector (SEC-OCD), which further unravels the heterogeneous structures of DOM in terms of molecular sizes (Huber et al. 2011, Quang et al. 2015). For example, biopolymer, quantified by SEC-OCD, is known to play an important role in membrane fouling potential (Ayache et al. 2013, Tian et al. 2013).

In this study, two advanced DOM analyzing tools, namely EEM-PARAFAC and SEC-OCD, are employed to track the changes of SMP composition in SBRs under different COD/N ratios. This study aims to (1) explore the changes in SMP composition in the effluent from biological treatment systems treating wastewater containing different COD/N ratios, and (2) examine the subsequent effects on UF membrane fouling potential. The results provide further insight into the efficacy of UF operation for the reclamation of wastewater with a range of COD/N ratios.

2 Materials and methods

2.1 Sequencing batch reactors

The initial mixed liquor suspended solids (MLSS) content was set to 4 g/L in each SBR. Three parallel sequencing batch reactors (SBRs) with a working volume of 2.4 L (total volume of 3 L) were continuously operated under a laboratory controlled conditions to simulate the activated sludge process. Each SBR was placed on a magnetic stirrer to agitate the MLSS and was aerated by an aquarium pump (Deakwang, South Korea) at an air flow rate of 120 L/h through an air stone diffuser to maintain the dissolved oxygen level from 4 to 6 mg/L. The mixed liquor pH and temperature were maintained at 7.5±0.5 and 25±1 ºC, respectively. The SBRs were fed every 24 hours with eight consecutive operational phases including filling (0.25 h), aeration (7 hours), mixing (1 hour), aeration (7 hours), mixing (1 hour), aeration (7 hours), settling (0.5 h), decanting (0.25 h) (Bernat et al. 2011). It is noteworthy that the MLSS value at each COD/N ratio varied slightly from the initial set point of 4 g/L. At steady state, the MLSS in the three SBRs were 4.3±0.2, 3.9±0.2 and 3.4±0.3 g/L responding to the COD/N ratio of 100/10, 100/5 and 100/2, respectively.

A volume (200 mL) of MLSS was wasted from each SBR during the last aeration phase of every cycle (or solid wasting rate of 200 mL/d) to maintain an SRT of 12 days. The calculation was based on the previous literature (Jarusutthirak and Amy 2007, Yu et al. 2015). In brief, the SRT, θ_c, can be calculated by the following equation:

$$\theta_c = \frac{VX}{F_w X_w} = \frac{V}{F_w} \quad (1)$$

where V is the effective volume of SBR (i.e., 2.4 L). F_w is the volume of mixed liquor withdrawn each day (0.2 L/d), and X_w and X are the MLSS concentrations in the mixed liquor (mg/L) and in the reactor (mg/L), respectively. The X_w and the X are identical for this study. In this study, the volumetric exchange rate (VER) was set at approximately 67%, equivalent to the hydraulic retention time (HRT) of 1.5 d. SBR effluent samples were collected each day and subsequently filtered through a 0.45 μm pore-sized membrane filter (acetate cellulose, Advantec, Japan) for SMP characterization. The effluent for UF membrane fouling experiments was collected at day 24^{th} and 25^{th} when the SBRs reached a steady state condition. The feed DOC concentrations for the COD/N ratios of 100/2, 100/5 and 100/10 were 7.15, 2.91 and 4.14 mgC/L, respectively.

Synthetic wastewater, comprising of glucose, nitrogen (NH_4Cl), phosphate (KH_2PO_4) and other trace elements, was used in this study. NH_4Cl content in the synthetic wastewater was varied to obtain three different COD/N ratios of 100/10, 100/5, and 100/2. They correspond to N rich (COD/N of 100/10), N medium (COD/N of 100/5), and N deficient (COD/N of 100/2) conditions, respectively (Tchobanoglous et al. 2003, Ye et al. 2011). A detail of other nutrient composition is shown in Table S1.

Activated sludge from a municipal wastewater treatment plant in Seoul, South Korea, was used to seed the SBRs. Before transferred to the lab scale SBRs, the seed activated sludge was acclimatized with the synthetic wastewater at COD/N of 100/5 for six weeks (Maqbool et al. 2015).

2.2 UF membrane filtration and the estimation of membrane fouling potential

A flat-sheet polyethersulfone (PES) membrane from Pall Corp. (USA) with the molecular weight cutoff (MWCO) of 30 kDa was used in this study. Polyethersulfone (PES) has been

commonly used for water treatment due to its high thermochemical resistance and endurance (Ahmad et al. 2013). The surface contact angle of the membrane, an indicator of hydrophobicity, was measured to be 57° (SmartDrop, Femtofab). Membrane zeta potential was -14 mV at pH 7.0 in 10 mM KCl solution (Qu et al. 2014). The membrane was stored in distilled and deionized water (DDW) for 48 hours before use. Additional cleaning was conducted by passing 2 L of DDW to remove any trace impurities in the membrane (Jermann et al. 2008).

A dead-end filtration experiment was performed using a 400 mL stirred cell Amicon 8400 UF unit (Millipore Corp., USA) with an effective filtration area of 41.8 cm^2. Nitrogen gas was used to pressurize the UF unit at 0.03 MPa. The water flux of the clean membrane was 113.5±4.25 $L/m^2/h$. A detailed description of the UF operation and extraction method for foulants is available in previous works (Ly et al. 2018, Quang et al. 2016). In brief, the UF filtration consisted of three cycles (i.e., 330 mL × 3 cycles), and each cycle was finished when the permeate solution reached a volume of 300 mL. The concentrate solution was considered as the remaining solution in the membrane (i.e., ~30 mL). The reversible foulant was obtained by hydraulic backwashing of the membrane sheets with 50 mL. At the end of the filtration, the membrane was soaking in a 0.1 N NaOH for 30 min in a shaker at 150 rpm. The pH of the irreversible foulant was re-adjusted by adding diluted HCl before spectroscopic measurements. Each UF experiment was conducted in duplicate.

The resistance-in-series model was used to calculate the absolute resistance following the equations below (Chiang and Cheryan 1986):

$$R_t = R_m + R_r + R_{ir} = \frac{TMP}{\mu J} \qquad (1)$$

where R_t ,R_m ,R_r ,and R_{ir} are the total hydraulic resistance (m^{-1}), the intrinsic membrane resistance (m^{-1}), the hydraulically reversible and irreversible resistance (m^{-1}), respectively. TMP is the transmembrane pressure (Pa). μ is the dynamic viscosity of the feed water (=0.001 Pa·s at 20 ºC), and J refers to the permeate flux (L/(m^2·h)).

R_m and R_t^n were determined by initial clean (deionized) water flux (J_o), and the solute flux, $J_{e(n)}$, at the end of n-cycle of filtration, respectively. R_m+R_{ir}^n was achieved by J_n, which is the flux obtained by filtering 200 mL deionized water after hydraulic backwashing. The n represents the number of filtration cycles.

$$R_m = \frac{TMP}{\mu J_o} \tag{2}$$

$$R_t^n = \frac{TMP}{\mu J_{e(n)}} \tag{3}$$

$$R_{ir}^n + R_m = \frac{TMP}{\mu J_n} \tag{4}$$

2.3 Analytical methods

2.3.1 Dissolved organic carbon (DOC) measurements and UV-visible spectroscopy

DOC concentrations were measured using a TOC analyzer (Shimadzu TOC-L, Japan). UV-Vis spectra were obtained at a wavelength range from 200 to 700 nm on a spectrophotometer (UV-1800, Shimadzu) with a 1-cm quartz cuvette. Specific UV absorbance (SUVA) values, an aromaticity indicator (Weishaar et al. 2003), were calculated by normalizing 100-fold UV absorption coefficient at 254 nm (UV_{254}) to DOC concentrations.

2.3.2 *Basic MLSS parameters*

MLSS was measured based on the Standard Methods (APHA 2005). Specific oxygen uptake rate (SOUR), an indicator for metabolic activity of sludge expressed by the unit of $mgO_2/gMLSS/h$. More than 300 mL of MLSS was poured in BOD bottles for the SOUR test. The dissolved oxygen (DO) was continuously recorded using a Nagivator DO meter (Forson Labs, USA) until the value reached 0 mg/L. SOUR was then determined by the slope of linear regression. The conductivity was measured using a SC82 conductivity meter (Yokogawa, Japan).

2.3.3 *Fluorescence EEM measurements and PARAFAC modeling*

Fluorescence EEM measurement was conducted using a luminescence spectrometer (Hitachi F-7000 FL, Japan) by scanning the emission wavelengths (Em) from 280 to 550 nm at 1 nm-increment and stepping through the excitation wavelengths (Ex) from 220 to 500 nm at 5 nm intervals. Excitation and emission slits were both adjusted at 10 nm. The scan speed was set at 12000 nm min^{-1}. To limit second order Raleigh scattering, a 290 nm cut off filter was used for all measurements. The fluorescence response to deionized water was subtracted from the EEM of each sample. The inner filter correction was neglected by sample dilution following the protocol described in (Kothawala et al. 2013). The fluorescence response to a blank solution (i.e., DDW) was subtracted from the EEM of each sample. Fluorescence intensity was normalized using Raman unit equivalents (RU) (Lawaetz and Stedmon 2009). PARAFAC modeling was conducted using MATLAB 7.1 (MathWorks, Natick, MA, USA) with the DOMFluor Toolbox (Stedmon and Bro 2008). Split half and residual analyses were applied to validate the identified components and their number.

2.3.4 *Size exclusion chromatography (SEC)*

A SEC system (Model 7, DOC-Labor, Germany), equipped with both organic carbon detector (OCD) and ultraviolet detector (UVD), was employed to compare the molecular weight (MW) distributions of SMP samples before and after UF (Huber et al. 2011). The 1000 µL volume of each SMP sample was injected at flow rate of 1.1 mL/min for a retention time of 130 min. Five different size fractions were quantified from the SEC chromatograms, which included biopolymer (BP) (i.e. >20kDa), humic substances (HS) (i.e. ~1kDa), building blocks (BB) (i.e. 300-500Da), low molecular weight acid (LMWA) (i.e. <350kDa), and low molecular weight neutral (LMWN) (i.e. <350kDa) according to the retention times (Huber et al. 2011). A separate SEC system with fluorescence detector was also utilized for this study to complement the results of EEM-PARAFAC. The system configuration is described in supplemental information (SI).

2.3.5 *Statistical analysis*

All statistical analyses were performed using the Origin Pro 8.6 software package. To validate the steady state condition in each SBRs, the standard deviations of bulk parameters (e.g., DOC and SUVA) were determined on the samples collected between day 15th and 25th (n = 10 × 3 reactors). Effects of COD/N on SMP (n = 45 for the acclimation period and n= 30 for the steady state) were validated using one-way ANOVA at 95% confidence for the steady state (Table 1).

3 Results and Discussion

3.1 *Variations of DOC and SUVA values of SMP with operation*

The temporal variations of DOC and SUVA values of SMP from all SBRs are shown in

Fig. 1. For all bioreactors, the DOC data showed an initial and sharp increase followed by some fluctuations. The DOC levels decreased afterwards until a stable period was reached with the relative variation of < 10%. A similar trend was also reported in another study (Esparza-Soto et al. 2011). The initial unstable period seems associated with the acclimatization of activated sludge microorganisms to the new environment. The sudden increase of SMP in the initial period can be ascribed to the secretion of polysaccharides and proteins from microbial communities to tolerate the metabolic stress (Wu et al. 2011). The highest DOC content was observed under the N deficient condition (COD/N ratio of 100/2) followed by the N rich condition (COD/N ratio of 100/10). The N medium condition (COD/N ratio of 100/5) led to the lowest DOC content in the effluent throughout the operation (Fig. 1). The average DOC concentrations at the stable period (i.e., after the 15th day of operation) were 7.5±0.5 mgC/L, 4.2±0.2 mgC/L, and 3.1±0.2 mgC/L, respectively (ANOVA $p<0.05$) (Table 1). The higher SMP levels at the N rich versus the N medium conditions were also reported by Ye et al. (2011), signifying the roles of COD/N ratio in governing the SMP concentrations within the bioreactor.

[FIGURE 1]

[TABLE 1]

Regardless of the COD/N ratios, SUVA values exhibited a consistent pattern in the trends of low levels for the first 7 days of operation, followed by general increases for the next 8 days and a plateau (i.e., a stable phase) for the rest (Fig. 1b). The SUVA values were higher with N enrichment, showing 2.9±0.1, 1.1±0.1 and 0.6±0.1 L/mgC-m for the stable phase at the COD/N ratios of 100/10, 100/5, and 100/2, respectively (ANOVA $p<0.05$). This phenomenon may be attributed to the differences in the synthetic pathways of proteins/polysaccharides at different COD/N ratios. Under the N rich condition, microorganisms could utilize excessive nitrogen to

produce more aromatic proteins and nucleic acids. In contrast, in the N deficient condition, they tend to produce more extracellular polysaccharides (i.e., non-aromatic structures) due to the lack of nitrogen for protein synthesis (Miqueleto et al. 2010, Wang et al. 2014, Ye et al. 2011). Other possible mechanisms may involve the secretion of soluble organic matter from sludge flocs under N deficiency to replenish the depleted nutrients (Hao et al. 2016) and/or to maintain endogenous respiration (Wu and Lee 2011). The N deficient condition might enhance the release of large size EPS enriched with polysaccharides into solution through sludge decay (Wu and Lee 2011). These mechanisms are in line with the decreasing biomass (i.e., MLSS) content under the N deficient condition in this study (Table 1). Similar observation has also been reported in the literature (Hao and Liao 2015, Roslev and King 1995). The MLSS concentrations at the steady state (i.e., after 15 day of operation) were 4.3±0.2, 3.9±0.2 and 3.4±0.3 mg/L for the COD/N ratios of 100/10, 100/5, and 100/2, respectively. The SEC-OCD chromatograms also supported the explanations as indicated by the higher DOC, but the lower UV responses for the BP fraction (i.e., more polysaccharides versus proteins) under the N deficient condition (Fig. S1).

3.2 Dynamic variations of individual FDOM components at different COD/N ratios

Three different FDOM components were identified by PARAFAC modeling (Fig. 2). Component 1 (C1), with two maxima at 230/340 nm and 280/340 nm (Ex/Em), can be assigned as tryptophan-like component based on previous literature (Maqbool et al. 2016, Yu et al. 2015). Component 2 (C2) has three peaks at 230/420 nm, 280/420 nm, and 340/420 nm (Ex/Em). These peaks are related to microbial fulvic-like peaks (Maqbool et al. 2016, Ni et al. 2010, Yu et al. 2015). The peaks of component 3 (C3), located at 240/460 nm, 280/460 nm, and 370/460 nm

(Ex/Em), are similar to those of microbial humic-like components reported in the literature (Li et al. 2008, Ni et al. 2010, Yu et al. 2015).

[FIGURE 2]

The fate of individual FDOM components in SMP was tracked at different COD/N ratios using the maximum fluorescence intensity (F_{max}) in the same protocol as in our previous works (Fig. 3) (Maqbool et al. 2017, Maqbool et al. 2016). Large variations were evident for all FDOM components during the acclimatization phase (i.e., before the 15th day of operation) at all COD/N ratios, followed by stable variations at the steady phase. Interestingly, the relative levels of the FDOM components at the steady state phase were dependent on the COD/N ratios as well as the type of the component. For example, the average level of C1 was the lowest at the N medium condition, while the lowest level of C3 was found under the N deficient condition (Fig. 3). In fact, the relatively high C1 under the N deficient condition is somewhat in contrast to the previous reports based on protein-bovine serum albumin content (Wang et al. 2014, Ye et al. 2011). This observation suggests that the C1 component may be derived not only from protein synthetic pathways but also from other sources (e.g., from cell lysis). This hypothesis is supported by the relatively low MLSS and/or SOUR values under the N deficiency at the steady phase compared to other conditions (Table 1). Following this, the fluorescence-detected SEC chromatograms of tryptophan-like C1 under the N deficient condition also suggest the exclusive presence of larger size molecules as evidenced by the signal at 280 nm/ 340 nm (Ex/Em) with a retention time of 4 minute compared to all other conditions (Fig. S2). It also well concurs with a previous report of (Li et al. 2008), who observed the fluorescence peaks of intracellular proteins similar to those of tryptophan-like component reported here. A recent study of Maqbool et al.

(2017) suggests that tryptophan-like C1 could be from the metabolisms of microorganisms in endogenous respiration (i.e. substrate deficiency).

[FIGURE 3]

The C2 component did not show apparent differences in the variations among the three COD/N ratios during the acclimatization period (Fig. 3b). At the steady state period, however, the N rich condition resulted in the highest levels of C2, which was well discriminated by the relatively low levels at the other two COD/N ratios (Fig. 3b). No difference in C2 was found between the N medium and deficient conditions at the steady state (ANOVA, $p>0.05$). In contrast, the microbial humic-like C3 exhibited clear distinctions in the levels, following the order of 100/10 > 100/5 > 100/2 at the COD/N ratios (Fig. 3c). Although it was reported that there was a close association between the enrichment of the humic-like component and microbial humification processes in biological treatment (Maqbool et al. 2016), it is not likely to be the sole mechanism to explain the observation of this study because of 1) no substantial increase of C2 or C3 over operation, 2) the relatively low MLSS, 3) the large amount of SMP discarded each cycle (i.e., VER = 67%), and 4) the relatively short SRT (12 days). Previous studies have shown that relatively long SRT might favor the accumulation of refractory humic/fulvic-like fluorophores (Esparza-Soto et al. 2011, Yu et al. 2015). For the alternative or additional mechanisms to produce the humic-like components other than microbial humification, it is worthy to note a previous study of Yu et al. (2010), who reported that both humic-like and fulvic-like fluorophores could be initially present in slime and loosely bound EPS, which could be released into supernatant as substrates during any endogenous phase to maintain cell activities (Geyik and Çeçen 2016, Wu and Lee 2011). This secretion can be further enhanced by the excessive addition of NH_4^+ (i.e., N rich condition) through the replacement with polyvalent

cations in EPS followed by the detachment of organic matter from EPS (Feng et al. 2012). This explanation is supported by the observation of a slightly higher conductivity measured in the SBR operated at the N rich condition as the indication of more presence of Ca^{2+} or Mg^{2+} (Table 1) and/or a higher amount of detached cells/cell fragments as shown in Fig. S3, which is caused by decreased EPS function as a backbone to aggregate bacterial cells, formation of flocs, biofilms and cell-cell adhesions (More et al. 2014).

3.3 Size distribution of SMP samples at different COD/N ratios

The SEC-OCD chromatograms indicated that size distribution of SMP was highly dependent on the COD/N ratio (Table 1, Fig. 4a). For example, BP was the most abundant fraction in SMP under the N deficient condition. Polysaccharides may be more dominant over proteins for the large molecular size because of the relatively low UV response compared to the high DOC at the corresponding retention times (Fig. S1). HS-like fraction became more dominant with a higher N ratio (Fig. 4a). For example, the relative distribution of HS-like fraction was 17.7%, 34.3%, and 38.7% at the COD/N ratios of 100/2, 100/5, and 100/10, respectively. Irrespective of the COD/N ratio, the size fractions of LMWA and LMWN showed very high UV responses in the SEC chromatograms (Fig. S1), which are consistent with the previous studies using glucose as a primary carbon feed source (Jarusutthirak and Amy 2007, Maqbool et al. 2017). These results suggest the significant presence of double-bonded small size amino acids in SMP samples.

[FIGURE 4]

3.4 Flux decline of UF and reversibility of SMP at different COD/N ratios

The UF fouling propensity of SMP samples was strongly affected by the COD/N ratio of the initial wastewater as shown in the extent of the flux decline following the order of the COD/N ratio of 100/2 > 100/10 > 100/5 (Fig. 5a). The normalized flux (J/J_o) at the end of filtration cycles corresponded to 0.26, 0.35, and 0.59 at the COD/N ratios of 100/2, 100/10, and 100/5, respectively. The relative order was the same as that of DOC levels at the steady state of operation (Table 1). These results are in agreement with many previous studies showing that higher levels of SMP led to a greater extent of membrane fouling (Ayache et al. 2013, Jarusutthirak and Amy 2006). Henderson et al. (2011) reported a strong correlation between membrane fouling and DOC concentrations of effluent wastewater during UF processes. The most severe total fouling resistance was observed at the low N condition (i.e., COD/N of 100/2), in which reversible fouling was much more responsible compared to other conditions (Fig. 5b). However, the relative contribution of irreversible fouling to the total fouling resistance was found to be the greatest under the N rich condition although it varied with the filtration cycles (Fig. 5b). The absolute values of the irreversible fouling at the end of the third cycle reached 13.7×10^{11}, 4.2×10^{11}, and 10.9×10^{11} (1/m) at the COD/N ratios of 100/10, 100/5, and 100/2, respectively. These results suggest that, not only SMP concentrations (i.e., DOC) but the chemical composition, which is governed by the COD/N ratio for this study, can also play an important role in determining the characteristics of membrane fouling.

[FIGURE 5]

3.5 Fate of different SMP constituents during UF

3.5.1 Removal rates of FDOM components in SMP at different COD/N ratios

The removal rates of three different fluorescent components were calculated based on the mass balance by multiplying the F_{max} values by the individual corresponding volumes of the feed and the permeate solutions (Quang et al. 2016, Yu et al. 2015). Irrespective of the COD/N ratio, the highest removal is observed for the tryptophan-like C1, followed by the fulvic-like C2 and the humic-like C3 (ANOVA, $p<0.05$) (Fig. 6a). For example, the removal rates of C1, C2 and C3 at the COD/N ratio of 100/10 were 68.2±1.9%, 15.6±2.5% and 14.4±1.9%, respectively. The results were comparable to those of a previous study (Maqbool et al. 2016) in which protein-like component was the most retained on membrane in a lab-scale membrane bioreactor (MBR) system. Proteinaceous biopolymers in domestic wastewater are commonly considered as one of the major foulants for low-pressure membrane filtration (Fan et al. 2008, Michael-Kordatou et al. 2015, Shon et al. 2006). In this study, the relatively lower removal rates of C2 and C3 are well supported by the fluorescence–detected SEC chromatograms (Fig S2), in which the molecular sizes of the fulvic/humic-like fluorophores were smaller than those of the tryptophan-like counterpart. These results are also consistent with previous reports (Maqbool et al. 2016, Meng et al. 2009) presenting a higher aromatic content of the permeate versus the feed solutions in MBR systems.

3.5.2 Characterization of FDOM components in SMP responsible for membrane fouling in UF

The mass balance approach was used to estimate the amounts of the individual FDOM components in the reversible and the irreversible solutions. The relative reversible fouling tendency of each fluorescent component was determined by the ratios of the amount of

component in the reversible solution to the total fouled amounts (Fig. 6b). The direct comparison across different fluorescent components was avoided here due to the concern over the differences in their quantum yields. For this study, C1 exhibited more contribution to the reversible versus the irreversible fouling compared to C2 and C3, with the relative contribution of >80% at all the COD/N ratios. In contrast, the relative contribution of C2 was lower than 40%, suggesting more association with irreversible fouling (Fig. 6b). The high affinity of C2 to irreversible fouling can be attributed to the small size molecules of the fluorescent component (Fig. S1), which may penetrate and adhere into membrane matrix and/or inner pores, resistant to hydraulic backwashing (Zhang et al. 2013).

[FIGURE 6]

The relative contribution of C3 to the reversible fouling tended to be higher with N enrichment (Fig. 6b). There are two possible explanations for the phenomenon. First, differences in COD/N ratios may render the alteration of the excreted organic matter composition during the cultivation of microorganisms. For example, Hao et al. (2016) found a carbon functional group (i.e., C=O stretch at 1735 cm^{-1}) uniquely present in activated sludge under N deficiency. The other possible explanation could be the additional origin of the humic-like component (C3) from the slime/bound EPS under the N rich condition. Potential differences in the characteristics of humic-like fluorophores between SMP and EPS have been reported in other literatures (Geng and Hall 2007, Wang et al. 2012).

3.5.3 Characterization of different size fractions in SMP responsible for membrane fouling in UF

Except for the irreversible solution at the N deficient condition, LMWN was found to be the most dominant size fraction present in both reversible and irreversible solutions followed by BP (Fig. 4). There was no contribution of HS fraction to membrane fouling. The exceptional case of the highest contribution of BP to the irreversible fouling at the COD/N ratio of 100/2 may be related to the most abundance of the size fraction in the SMP solution. For example, the concentrations of BP fraction in feed solutions were 862 μgC/L at the COD/N ratio of 100/2 as compared to 146 μgC/L and 105 μgC/L at the ratios of 100/10 and 100/5 (Table 1). The significant contribution of LMWN in the irreversible fouling could be explained by the adhesion property of LMWN for the PES membrane materials via hydrophobic interactions.

The significant presence of low molecular sized fractions (i.e., LMWN) in the reversible solutions could be explained by the operation of the cake/gel layer serving as an additional clarifier before membrane filtration (Qu et al. 2014, Villacorte et al. 2015). Another possibility may lie in the dominance of the amino acids in LMWN fraction, which can exhibit negatively charges at neutral conditions (Gallardo et al. 1991), generating the repulsive forces with the membrane surface. Meanwhile, the substantial contribution of the large size BP to reversible fouling can be attributed to size exclusion in the form of cake/gel layer, which is easily detached by hydraulic backwashing (Guo et al. 2012, Lin et al. 2009). Besides, chemical interactions may also be involved for membrane fouling. For example, the hydrophilic nature of BP (e.g., polysaccharides and proteins) (Matilainen et al. 2010) could render a lesser degree of the adhesion onto PES membrane.

It is noteworthy that different COD/N ratio alters the chemical composition of SMP, thus influencing the types and the characteristics of the foulants (i.e., membrane fouling behavior). For example, proteinaceous BP, which exhibits relatively higher UV signals in SEC than polysaccharides, contributed more to reversible fouling at the N deficient condition (i.e., COD/N ratio of 100/2), while its contribution to irreversible fouling was much smaller compared to other N richer conditions (Fig. S1). Regardless of COD/N ratio, HS-like size fraction was not found in either fouling solutions, which contrasted with significant contributions of C2 or C3 components in fouling solutions (Fig. 6 and Table S2). The limited data of this study makes it difficult to unravel the unexplained observation. Further work should be carried out to explore the linkage between the fate of HS size fraction and humic-like FDOM components in similar treatment systems.

4 Conclusions

The tracking of three independent fluorescent components and different size fractions of SMP allowed to obtain an understanding of the differences in SMP composition at varying COD/N ratios. SMPs produced at the N medium condition resulted in the lowest DOC concentrations and thus the least degree on membrane fouling, highlighting the importance of balancing COD/N ratio for the post UF processes. Protein-like C1 and fulvic-like C2 were most associated with reversible and irreversible fouling, respectively, suggesting that each fluorescent component could serve as a spectroscopic surrogate to predict the characteristics of UF membrane fouling. The reversible extent of humic-like C3 was greater with higher COD/N ratios. The HS-like size fraction was not involved in membrane fouling, which contrasted with

the behavior of fulvic/humic-like FDOM, suggesting the potential concern for the size fraction-related water quality (e.g., formation of disinfection byproducts) in the permeate after the post UF processes. Our study provided further insight into the changes in SMP composition and subsequent effects on fouling characteristics of post UF processes upon varying COD/N ratios in wastewater.

Acknowledgements

This work was supported by a National Research Foundation of Korea (NRF) grant funded by the Korean government (MSIP) (No. 2017R1A2A2A09069617).

References

Ahmad, A.L., Abdulkarim, A.A., Ooi, B.S. and Ismail, S. (2013) Recent development in additives modifications of polyethersulfone membrane for flux enhancement. Chem. Eng. J. 223, 246-267.doi: http://doi.org/10.1016/j.cej.2013.02.130

APHA, A., WEF (2005) Standard Methods for the Examination of Water and Wastewater, 21st ed. American Public Health Association, Washington, DC.

Ayache, C., Pidou, M., Croué, J.P., Labanowski, J., Poussade, Y., Tazi-Pain, A., Keller, J. and Gernjak, W. (2013) Impact of effluent organic matter on low-pressure membrane fouling in tertiary treatment. Water Res. 47(8), 2633-2642.doi: http://dx.doi.org/10.1016/j.watres.2013.01.043

Bernat, K., Kulikowska, D., Zielińska, M., Cydzik-Kwiatkowska, A. and Wojnowska-Baryła, I. (2011) Nitrogen removal from wastewater with a low COD/N ratio at a low oxygen concentration. Bioresour. Technol. 102(7), 4913-4916.doi: http://doi.org/10.1016/j.biortech.2010.12.116

Chiang, B.H. and Cheryan, M. (1986) Ultrafiltration of Skimmilk in Hollow Fibers. J. Food Sci. 51(2), 340-344.doi: 10.1111/j.1365-2621.1986.tb11124.x

Chon, K., KyongShon, H. and Cho, J. (2012) Membrane bioreactor and nanofiltration hybrid system for reclamation of municipal wastewater: Removal of nutrients, organic matter and micropollutants. Bioresour. Technol. 122, 181-188.doi: http://dx.doi.org/10.1016/j.biortech.2012.04.048

Esparza-Soto, M., Núñez-Hernández, S. and Fall, C. (2011) Spectrometric characterization of effluent organic matter of a sequencing batch reactor operated at three sludge retention times. Water Res. 45(19), 6555-6563.doi: http://doi.org/10.1016/j.watres.2011.09.057
Fan, L., Nguyen, T., Roddick, F.A. and Harris, J.L. (2008) Low-pressure membrane filtration of secondary effluent in water reuse: Pre-treatment for fouling reduction. J. Membr. Sci. 320(1–2), 135-142.doi: http://dx.doi.org/10.1016/j.memsci.2008.03.058
Feng, S., Zhang, N., Liu, H., Du, X., Liu, Y. and Lin, H. (2012) The effect of COD/N ratio on process performance and membrane fouling in a submerged bioreactor. Desalination 285, 232-238.doi: http://doi.org/10.1016/j.desal.2011.10.008
Gallardo, V., Bolívar, M., Salcedo, J. and Delgado, A.V. (1991) Trends in Colloid and Interface Science V. Corti, M. and Mallamace, F. (eds), pp. 447-455, Steinkopff, Heidelberg.
Geng, Z. and Hall, E.R. (2007) A comparative study of fouling-related properties of sludge from conventional and membrane enhanced biological phosphorus removal processes. Water Res. 41(19), 4329-4338.doi: http://dx.doi.org/10.1016/j.watres.2007.07.007
Geyik, A.G. and Çeçen, F. (2016) Production of protein- and carbohydrate-EPS in activated sludge reactors operated at different carbon to nitrogen ratios. J. Chem. Technol. Biotechnol. 91(2), 522-531.doi: 10.1002/jctb.4608
Guo, W., Ngo, H.-H. and Li, J. (2012) A mini-review on membrane fouling. Bioresour. Technol. 122(0), 27-34.doi: http://dx.doi.org/10.1016/j.biortech.2012.04.089
Hao, L. and Liao, B.Q. (2015) Effect of organic matter to nitrogen ratio on membrane bioreactor performance. Environ. Technol. 36(20), 2674-2680.doi: 10.1080/09593330.2015.1043353
Hao, L., Liss, S.N. and Liao, B.Q. (2016) Influence of COD:N ratio on sludge properties and their role in membrane fouling of a submerged membrane bioreactor. Water Res. 89, 132-141.doi: http://doi.org/10.1016/j.watres.2015.11.052
Henderson, R.K., Baker, A., Murphy, K.R., Hambly, A., Stuetz, R.M. and Khan, S.J. (2009) Fluorescence as a potential monitoring tool for recycled water systems: A review. Water Res. 43(4), 863-881.doi: http://dx.doi.org/10.1016/j.watres.2008.11.027
Henderson, R.K., Subhi, N., Antony, A., Khan, S.J., Murphy, K.R., Leslie, G.L., Chen, V., Stuetz, R.M. and Le-Clech, P. (2011) Evaluation of effluent organic matter fouling in ultrafiltration treatment using advanced organic characterisation techniques. J. Membr. Sci. 382(1–2), 50-59.doi: http://dx.doi.org/10.1016/j.memsci.2011.07.041
Huber, S.A., Balz, A., Abert, M. and Pronk, W. (2011) Characterisation of aquatic humic and non-humic matter with size-exclusion chromatography - organic carbon detection - organic nitrogen detection (LC-OCD-OND). Water Res. 45(2), 879-885.doi:
Ishii, S.K.L. and Boyer, T.H. (2012) Behavior of Reoccurring PARAFAC Components in Fluorescent Dissolved Organic Matter in Natural and Engineered Systems: A Critical Review. Environ. Sci. Technol. 46(4), 2006-2017.doi: 10.1021/es2043504
Jarusutthirak, C. and Amy, G. (2006) Role of Soluble Microbial Products (SMP) in Membrane Fouling and Flux Decline. Environ. Sci. Technol. 40(3), 969-974.doi: 10.1021/es050987a
Jarusutthirak, C. and Amy, G. (2007) Understanding soluble microbial products (SMP) as a component of effluent organic matter (EfOM). Water Res. 41(12), 2787-2793.doi: http://doi.org/10.1016/j.watres.2007.03.005
Jermann, D., Pronk, W., Kägi, R., Halbeisen, M. and Boller, M. (2008) Influence of interactions between NOM and particles on UF fouling mechanisms. Water Res. 42(14), 3870-3878.doi: http://dx.doi.org/10.1016/j.watres.2008.05.013

Kothawala, D.N., Murphy, K.R., Stedmon, C.A., Weyhenmeyer, G.A. and Tranvik, L.J. (2013) Inner filter correction of dissolved organic matter fluorescence. Limnol. Oceanogr. Methods 11(12), 616-630.doi: 10.4319/lom.2013.11.616
Lawaetz, A.J. and Stedmon, C.A. (2009) Fluorescence Intensity Calibration Using the Raman Scatter Peak of Water. Appl. Spectrosc. 63(8), 936-940.doi: doi:10.1366/000370209788964548
Li, P. and Hur, J. (2017) Utilization of UV-Vis spectroscopy and related data analyses for dissolved organic matter (DOM) studies: A review. Crit. Rev. Environ. Sci. Technol., 0-0.doi: 10.1080/10643389.2017.1309186
Li, W.-H., Sheng, G.-P., Liu, X.-W. and Yu, H.-Q. (2008) Characterizing the extracellular and intracellular fluorescent products of activated sludge in a sequencing batch reactor. Water Res. 42(12), 3173-3181.doi: https://doi.org/10.1016/j.watres.2008.03.010
Lin, C.-F., Yu-Chen Lin, A., Sri Chandana, P. and Tsai, C.-Y. (2009) Effects of mass retention of dissolved organic matter and membrane pore size on membrane fouling and flux decline. Water Res. 43(2), 389-394.doi: http://dx.doi.org/10.1016/j.watres.2008.10.042
Ly, Q.V., Kim, H.-C. and Hur, J. (2018) Tracking fluorescent dissolved organic matter in hybrid ultrafiltration systems with TiO2/UV oxidation via EEM-PARAFAC. J. Membr. Sci.doi: https://doi.org/10.1016/j.memsci.2017.12.020
Maeng, S.K., Timmes, T.C. and Kim, H.C. (2015) Characterization of EfOM fraction responsible for short-term fouling in ultrafiltration. Chemosphere 50, 2697-2707.
Maqbool, T., Cho, J. and Hur, J. (2017) Dynamic changes of dissolved organic matter in membrane bioreactors at different organic loading rates: Evidence from spectroscopic and chromatographic methods. Bioresour. Technol. 234, 131-139.doi: http://doi.org/10.1016/j.biortech.2017.03.035
Maqbool, T., Khan, S.J., Waheed, H., Lee, C.-H., Hashmi, I. and Iqbal, H. (2015) Membrane biofouling retardation and improved sludge characteristics using quorum quenching bacteria in submerged membrane bioreactor. J. Membr. Sci. 483, 75-83.doi: http://dx.doi.org/10.1016/j.memsci.2015.02.011
Maqbool, T., Quang, V.L., Cho, J. and Hur, J. (2016) Characterizing fluorescent dissolved organic matter in a membrane bioreactor via excitation–emission matrix combined with parallel factor analysis. Bioresour. Technol. 209, 31-39.doi: http://dx.doi.org/10.1016/j.biortech.2016.02.089
Matilainen, A., Vepsäläinen, M. and Sillanpää, M. (2010) Natural organic matter removal by coagulation during drinking water treatment: A review. Adv. Colloid Interface Sci. 159(2), 189-197.doi: http://dx.doi.org/10.1016/j.cis.2010.06.007
Meng, F., Drews, A., Mehrez, R., Iversen, V., Ernst, M., Yang, F., Jekel, M. and Kraume, M. (2009) Occurrence, Source, and Fate of Dissolved Organic Matter (DOM) in a Pilot-Scale Membrane Bioreactor. Environ. Sci. Technol. 43(23), 8821-8826.doi: 10.1021/es9019996
Michael-Kordatou, I., Michael, C., Duan, X., He, X., Dionysiou, D.D., Mills, M.A. and Fatta-Kassinos, D. (2015) Dissolved effluent organic matter: Characteristics and potential implications in wastewater treatment and reuse applications. Water Res. 77(0), 213-248.doi: http://dx.doi.org/10.1016/j.watres.2015.03.011
Miqueleto, A.P., Dolosic, C.C., Pozzi, E., Foresti, E. and Zaiat, M. (2010) Influence of carbon sources and C/N ratio on EPS production in anaerobic sequencing batch biofilm reactors for wastewater treatment. Bioresour. Technol. 101(4), 1324-1330.doi: http://doi.org/10.1016/j.biortech.2009.09.026

More, T.T., Yadav, J.S.S., Yan, S., Tyagi, R.D. and Surampalli, R.Y. (2014) Extracellular polymeric substances of bacteria and their potential environmental applications. J. Environ. Manage. 144, 1-25.doi: 10.1016/j.jenvman.2014.05.010
Ni, B.-J., Fang, F., Xie, W.-M., Sun, M., Sheng, G.-P., Li, W.-H. and Yu, H.-Q. (2009) Characterization of extracellular polymeric substances produced by mixed microorganisms in activated sludge with gel-permeating chromatography, excitation–emission matrix fluorescence spectroscopy measurement and kinetic modeling. Water Res. 43(5), 1350-1358.doi: http://dx.doi.org/10.1016/j.watres.2008.12.004
Ni, B.-J., Zeng, R.J., Fang, F., Xie, W.-M., Sheng, G.-P. and Yu, H.-Q. (2010) Fractionating soluble microbial products in the activated sludge process. Water Res. 44(7), 2292-2302.doi: http://doi.org/10.1016/j.watres.2009.12.025
Qu, F., Liang, H., Zhou, J., Nan, J., Shao, S., Zhang, J. and Li, G. (2014) Ultrafiltration membrane fouling caused by extracellular organic matter (EOM) from Microcystis aeruginosa: Effects of membrane pore size and surface hydrophobicity. J. Membr. Sci. 449(0), 58-66.doi: http://dx.doi.org/10.1016/j.memsci.2013.07.070
Quang, V.L., Choi, I. and Hur, J. (2015) Tracking the behavior of different size fractions of dissolved organic matter in a full-scale advanced drinking water treatment plant. Environ. Sci. Pollut. Res. 22(22), 18176-18184.doi: 10.1007/s11356-015-5040-3
Quang, V.L., Kim, H.-C., Maqbool, T. and Hur, J. (2016) Fate and fouling characteristics of fluorescent dissolved organic matter in ultrafiltration of terrestrial humic substances. Chemosphere 165, 126-133.doi: http://dx.doi.org/10.1016/j.chemosphere.2016.09.029
Roslev, P. and King, G.M. (1995) Aerobic and anaerobic starvation metabolism in methanotrophic bacteria. Appl. Environ. Microbiol. 61(4), 1563-1570.doi:
Shon, H.K., Vigneswaran, S., Kim, I.S., Cho, J. and Ngo, H.H. (2006) Fouling of ultrafiltration membrane by effluent organic matter: A detailed characterization using different organic fractions in wastewater. J. Membr. Sci. 278(1–2), 232-238.doi: http://dx.doi.org/10.1016/j.memsci.2005.11.006
Stedmon, C.A. and Bro, R. (2008) Characterizing dissolved organic matter fluorescence with parallel factor analysis: a tutorial. Limnol. Oceanogr. Methods 6(11), 572-579.doi: 10.4319/lom.2008.6.572
Tchobanoglous, G., Burton, F. and Stensel, H. (2003) Wastewater engineering: treatment and reuse, New York, NY: Mc Graw-Hill Higher Education.
Tian, J.-y., Ernst, M., Cui, F. and Jekel, M. (2013) Correlations of relevant membrane foulants with UF membrane fouling in different waters. Water Res. 47(3), 1218-1228.doi: http://dx.doi.org/10.1016/j.watres.2012.11.043
Tian, Y., Chen, L., Zhang, S. and Zhang, S. (2011) A systematic study of soluble microbial products and their fouling impacts in membrane bioreactors. Chem. Eng. J. 168(3), 1093-1102.doi: http://dx.doi.org/10.1016/j.cej.2011.01.090
Villacorte, L.O., Ekowati, Y., Winters, H., Amy, G., Schippers, J.C. and Kennedy, M.D. (2015) MF/UF rejection and fouling potential of algal organic matter from bloom-forming marine and freshwater algae. Desalination 367(0), 1-10.doi: http://dx.doi.org/10.1016/j.desal.2015.03.027
Wang, Q., Wang, Z., Wu, Z., Ma, J. and Jiang, Z. (2012) Insights into membrane fouling of submerged membrane bioreactors by characterizing different fouling layers formed on membrane surfaces. Chem. Eng. J. 179, 169-177.doi: http://dx.doi.org/10.1016/j.cej.2011.10.074

Wang, Z., Gao, M., Xin, Y., Ma, D., She, Z., Wang, Z., Sun, C. and Ren, Y. (2014) Effect of C/N ratio on extracellular polymeric substances of activated sludge from an anoxic–aerobic sequencing batch reactor treating saline wastewater. Environ. Technol. 35(22), 2821-2828.doi: 10.1080/09593330.2014.924563
Weishaar, J.L., Aiken, G.R., Bergamaschi, B.A., Fram, M.S., Fujii, R. and Mopper, K. (2003) Evaluation of Specific Ultraviolet Absorbance as an Indicator of the Chemical Composition and Reactivity of Dissolved Organic Carbon. Environ. Sci. Technol. 37(20), 4702-4708.doi: 10.1021/es030360x
Wu, B., Yi, S. and Fane, A.G. (2011) Microbial community developments and biomass characteristics in membrane bioreactors under different organic loadings. Bioresour. Technol. 102(13), 6808-6814.doi: https://doi.org/10.1016/j.biortech.2011.04.012
Wu, S.C. and Lee, C.M. (2011) Correlation between fouling propensity of soluble extracellular polymeric substances and sludge metabolic activity altered by different starvation conditions. Bioresour. Technol. 102(9), 5375-5380.doi: http://doi.org/10.1016/j.biortech.2010.11.093
Ye, F., Ye, Y. and Li, Y. (2011) Effect of C/N ratio on extracellular polymeric substances (EPS) and physicochemical properties of activated sludge flocs. J. Hazard. Mater. 188(1-3), 37-43.doi: 10.1016/j.jhazmat.2011.01.043
Yu, G.-H., He, P.-J. and Shao, L.-M. (2010) Novel insights into sludge dewaterability by fluorescence excitation–emission matrix combined with parallel factor analysis. Water Res. 44(3), 797-806.doi: http://dx.doi.org/10.1016/j.watres.2009.10.021
Yu, H., Qu, F., Sun, L., Liang, H., Han, Z., Chang, H., Shao, S. and Li, G. (2015) Relationship between soluble microbial products (SMP) and effluent organic matter (EfOM): Characterized by fluorescence excitation emission matrix coupled with parallel factor analysis. Chemosphere 121, 101-109.doi: http://dx.doi.org/10.1016/j.chemosphere.2014.11.037
Zhang, X., Fan, L. and Roddick, F.A. (2013) Understanding the fouling of a ceramic microfiltration membrane caused by algal organic matter released from Microcystis aeruginosa. J. Membr. Sci. 447(0), 362-368.doi: http://dx.doi.org/10.1016/j.memsci.2013.07.059

Table 1. Key SMP parameters of the steady state (after the 15th day of operation) at three different COD/N ratios (average ± standard deviation of 10 samples)

	100/10 (N rich)	**100/5 (N medium)**	**100/2 (N deficient)**
Glucose/NH_4Cl (g/g)	3.75/1.53	3.75/0.76	3.75/0.3
MLSS (g/L)	4.3±0.2	3.9±0.2	3.4±0.3
Conductivity (mS/cm)	30.2±4.9	23.4±6.0	20.9±6.4

SOUR (mg/L)	4.5±0.2	3.1±0.2	3.4±0.3
DOC (mgC/L)	4.2±0.2	3.1±0.2	7.5±0.5
SUVA (L/mgC-m)	2.9±0.1	1±0.1	0.6±0.1
BP* (µgC/L)	146	105	862
HS* (µgC/L)	347	281	332
BB* (µgC/L)	78	276	261
LMWN* (µgC/L)	271	132	401
LMWA* (µgC/L)	53	25	19

Note: the SEC based on the SMP with four time dilution and was taken at day 24th and 25th.

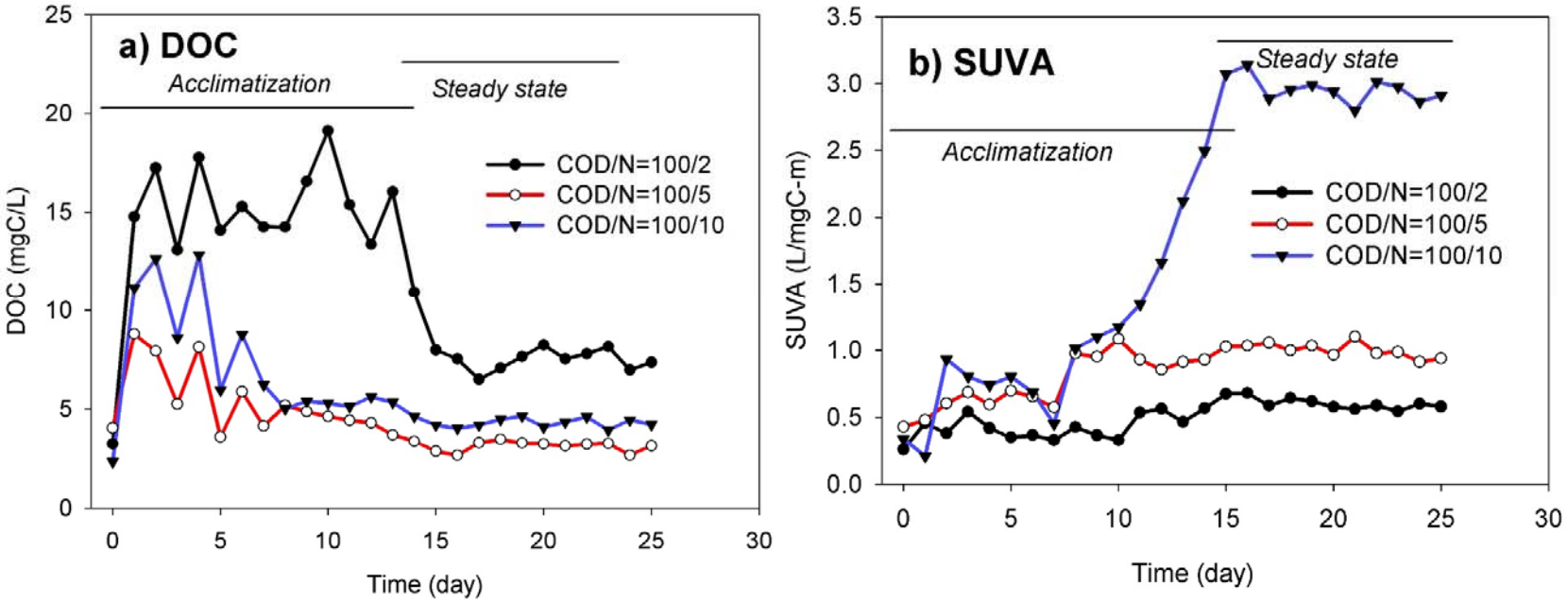

Fig. 1. Dynamic variations in SMP produced in sequence batch bioreactors under different COD/N ratios in terms of a) DOC and b) SUVA values

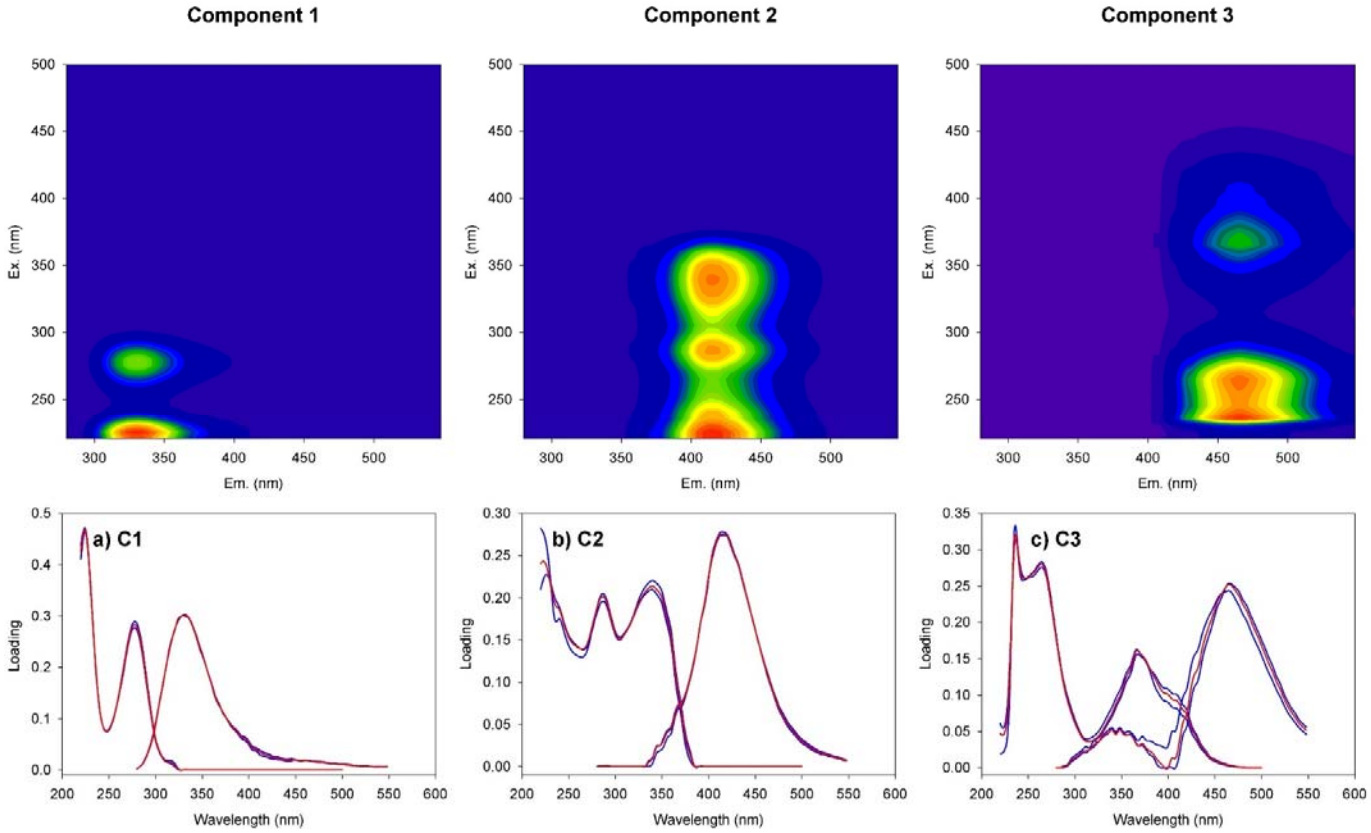

Fig. 2. EEM-PARAFAC model output showing three identified fluorescent components (above) and the corresponding excitation/emission loadings (below). Excitation/emission loadings consist of two independent halves of the dataset (blue lines) and the complete dataset (red lines).

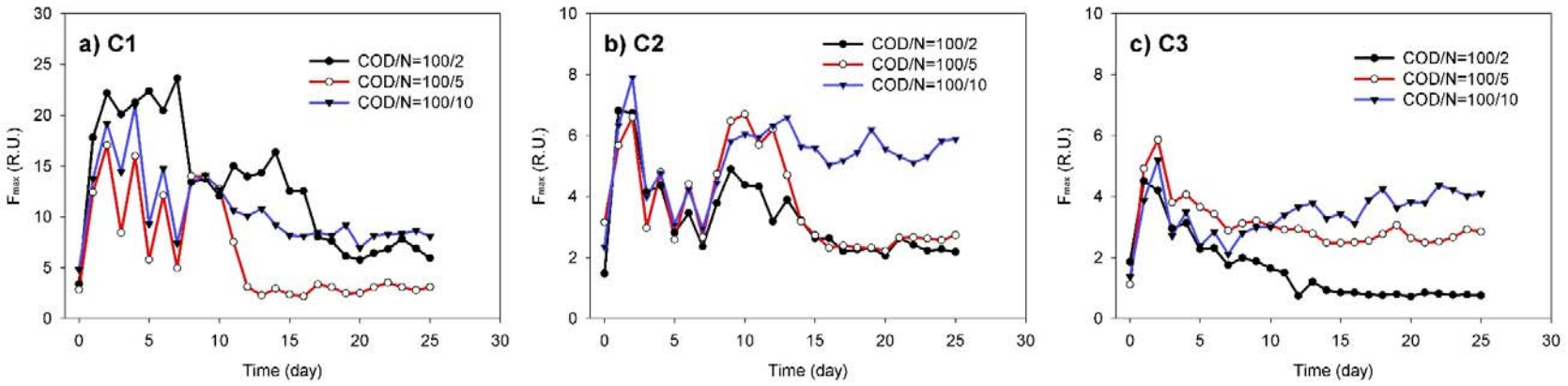

Fig. 3. Dynamic variations in fluorescent components of SMP at different COD/N ratios. a) Protein-like component C1, b) Fulvic-like component C2, and c) Humic-like component C3

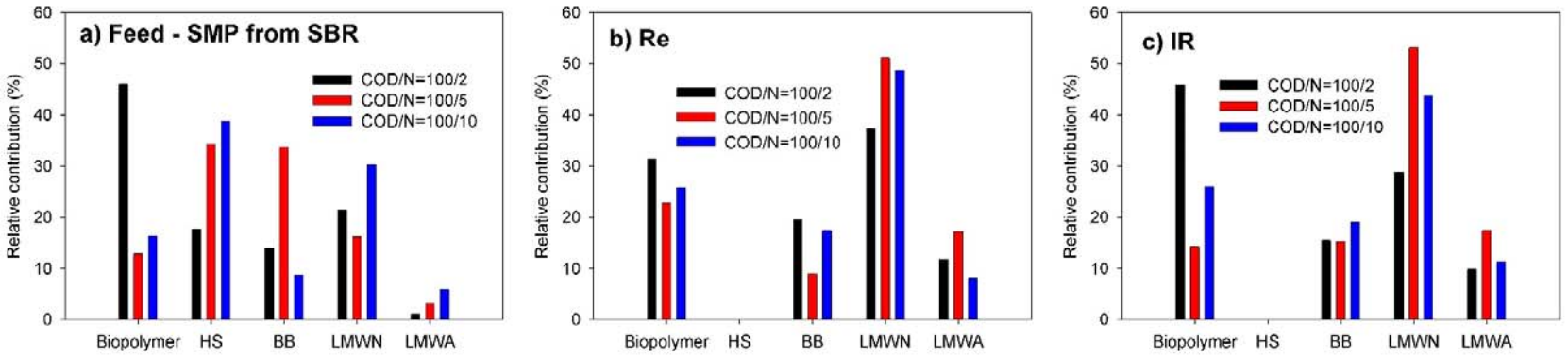

Fig. 4. Relative contributions of different SMP size fractions at different COD/N ratios detected by SEC-OCD in a) feed solutions-SMP from SBR, b) reversible solutions, and c) irreversible solutions

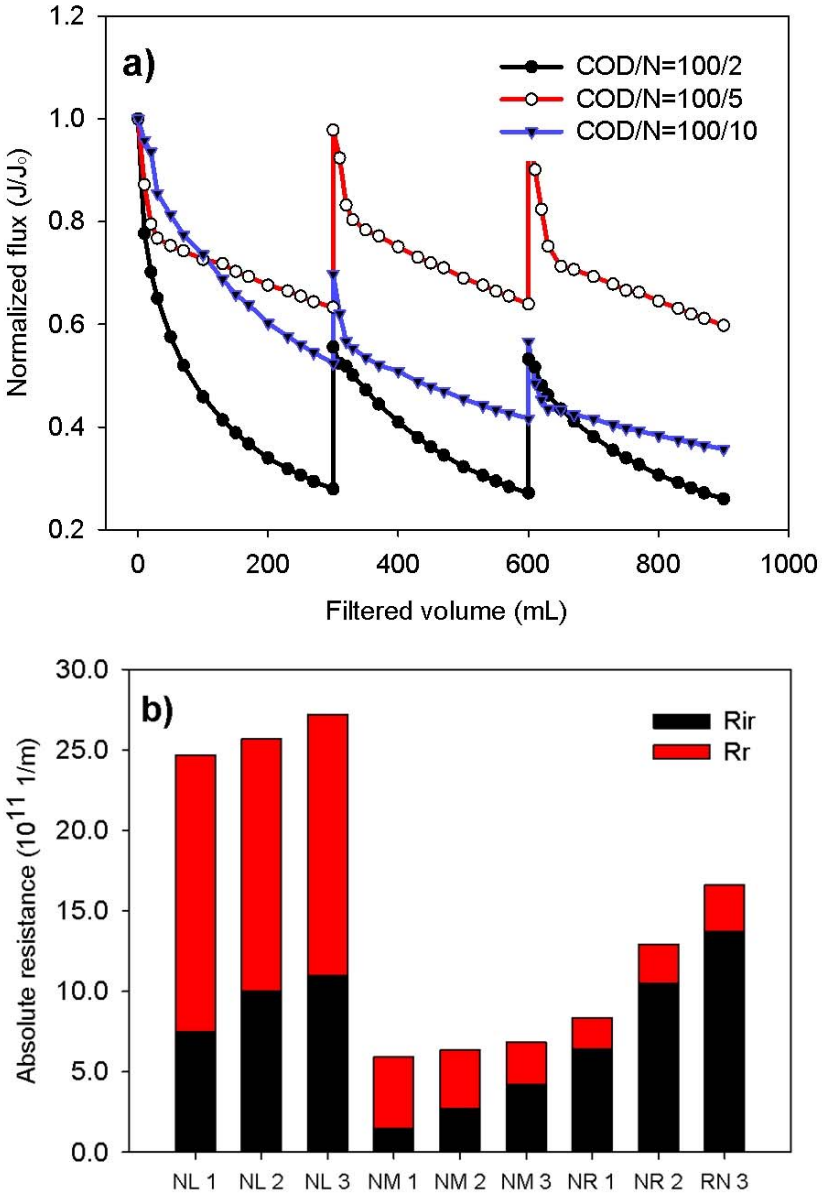

Fig. 5. Influence of COD/N ratio on membrane fouling potential by SMP as revealed by a) flux decline and b) absolute resistance. NL, NM and NR in Fig. 5b refer to the nitrogen low condition (COD/N ratio of 100/2), the nitrogen medium condition (COD/N ratio of 100/5), and the nitrogen rich condition (COD/N ratio of 100/10), respectively, with the number of filtration cycles. R_{ir} and R_r are calculated based on Equation (1), (2), (3) and (4) in the main text.

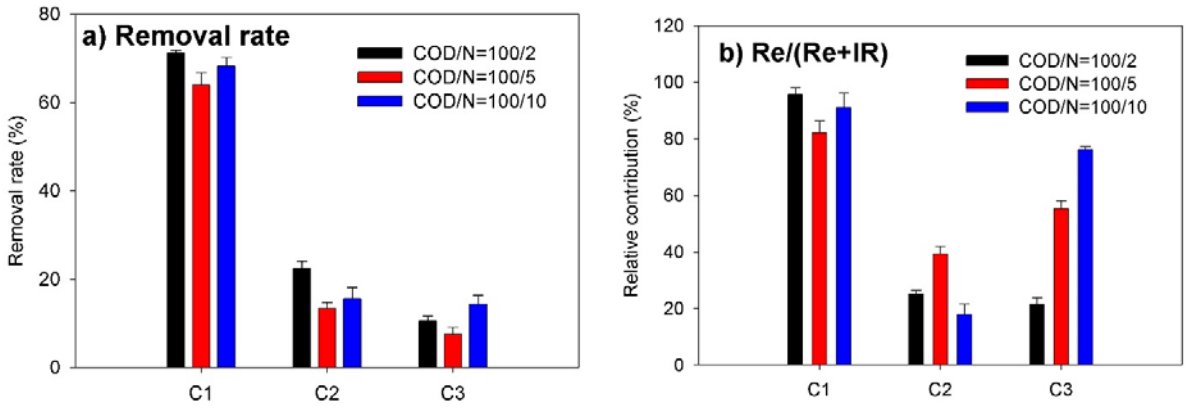

Fig. 6. Effects of COD/N ratios on the fate of different SMP fluorescent components in terms of a) the removal rates, and b) the relative contribution to reversible membrane fouling potential (Please note that the sum of the relative contributions (C1, C2, and C3) is not 100% because the calculation was based on the individual fluorescent component).

29